Proceedings of the Seventh IASTED International Conference
POWER AND ENERGY SYSTEMS
August 29–31, 2007, Palma de Mallorca, Spain
ISBN Hardcopy: 978-0-88986-689-8 / CD: 978-0-88986-690-4

DEVELOPMENT OF A CLOSED-LOOP POWER CONTROL FOR A DYNAMIC INTERPHASE POWER FLOW CONTROLLER BASED ON A FUNDAMENTAL COMPONENT MODEL

Ebner G., Trunk K., Herold G.
UNIVERSITY of ERLANGEN-NUREMBERG
Institute of Electrical Power Systems
Cauerstrasse 4, Bldg. 1
D-91058 Erlangen
Germany
E-Mail: ebner@eev.eei.uni-erlangen.de
kai_trunk@web.de
herold@eev.eei.uni-erlangen.de

ABSTRACT

This paper describes the development of a closed-loop power control for a Dynamic Interphase Power Flow Conroller (DIPFC). A DIPFC is a thyristor switched device within the FACTS family. In the following analysis the DIPFC is connected in series to a transmission line which links up two power grids in order to have an effect on the transmitted active- and reactive power.
In [1] it was pointed out that under certain neglects the effects of the DIPFC on the electric circuit can be expressed by fundamental component susceptances of the thyristor switched modules. Another previous research project [2] demonstrated that a DIPFC device makes it possible to control the active- and reactive-power flow independently from each other.
This paper in hand shows the development of a closed-loop power control for a DIPFC with two controlled modules in order to realize the above mentioned possibility.

KEY WORDS

FACTS, DIPFC, Power Transmission, IPC, IPFC

1. Introduction

In the last decade the electrical energy market was subject to significant changes. The liberalisation led to an increasing demand for a defined exchange of electrical power. Several types of FACTS were developed in order to control the active- and reactive-power flow or to enhance voltage and system stability. The DIPFC presented in this paper allows the independently controlled exchange of active- and reactive power between two arbitrary network nodes.

2. Analysed System

At first the analysed system is presented and basic possibilities of influencing the power transmission over a transmission line using a DIPFC are shown. Figure 1 depicts the 3-phase circuit diagram of the DIPFC. Left and right to the shown DIPFC structure (nodes *i* and *k*) two electric power grids can be connected. The device is built up out of two TCSC modules. All elements B_1 and B_2 have the principle structure of a Thyristor Controlled Series Capacitor (TCSC) depicted in figure 2. In this investigation the modules are described by their variable fundamental component susceptances B_1 and B_2.

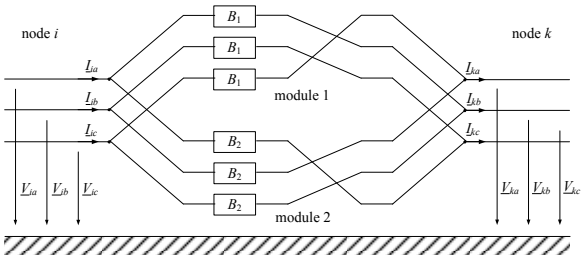

Fig. 1: 3-phase circuit diagram of the DIPFC

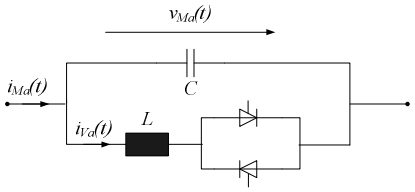

Fig. 2: Structure of a Thyristor Controlled Series Capacitor

A transformation of the 3-phase structure into symmetrical components leads to the equivalent circuit of the positive-sequence system, shown in figure 3. The connected grids are described by their short circuit impedances and open-circuit voltages.

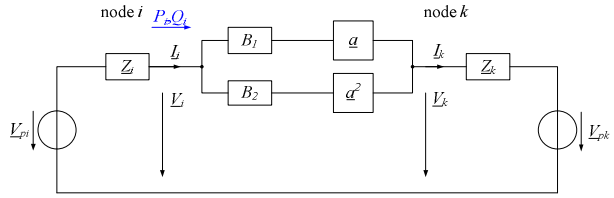

Fig. 3: Positive-sequence system equivalent circuit of the investigated system

3. Optimal parameters for the power exchange

An analysis of this equivalent circuit provides the necessary equation of the transmitted active- and reactive power (P_i and Q_i) as a function of the two susceptances (B_1, B_2) in which the parameters k and δ express the proportion of magnitudes and the difference of phase angles of the voltages $\underline{V}_i$ and $\underline{V}_k$.
The complex power on the network node i is the sum of the power which flows through the two modules.

$$\underline{S}_{i1} = \frac{3V_i^2}{X_1}\left(k\cdot\sin\left(\frac{2\pi}{3}-\delta\right)+\mathrm{j}\left(1-k\cos\left(\frac{2\pi}{3}-\delta\right)\right)\right) \quad (1)$$

with: $k = \frac{|\underline{V}_i|}{|\underline{V}_k|}$ and $\delta = \arg\left(\frac{\underline{V}_i}{\underline{V}_k}\right)$

$$\underline{S}_{i2} = \frac{3V_i^2}{X_2}\left(-k\cdot\sin\left(\frac{2\pi}{3}+\delta\right)+\mathrm{j}\left(1-k\cos\left(\frac{2\pi}{3}+\delta\right)\right)\right) \quad (2)$$

If the complex power is separated in its two orthogonal parts, the active- and reactive power can be expressed as:

$$P_i = 3V_i^2\left(\frac{k\sin\left(\frac{2\pi}{3}-\delta\right)}{X_1}-\frac{k\sin\left(\frac{2\pi}{3}+\delta\right)}{X_2}\right) \quad (3)$$

$$Q_i = 3V_i^2\left(\frac{1-k\cos\left(\frac{2\pi}{3}-\delta\right)}{X_1}-\frac{1-k\cos\left(\frac{2\pi}{3}+\delta\right)}{X_2}\right) \quad (4)$$

Because there is an unsteady point at the description of the fundamental impedance as a function of the ignition angle, the modules will be described with their susceptances. Equations (3) and (4) can be expressed by a matrix:

$$\begin{pmatrix}P_i\\Q_i\end{pmatrix} = 3V_i^2\mathbf{A}\begin{pmatrix}B_1\\B_2\end{pmatrix} \quad \text{where:}$$

$$\mathbf{A}=\begin{pmatrix}-k\sin\left(\frac{2\pi}{3}-\delta\right) & +k\sin\left(\frac{2\pi}{3}+\delta\right)\\ -1+k\cos\left(\frac{2\pi}{3}-\delta\right) & -1+k\cos\left(\frac{2\pi}{3}+\delta\right)\end{pmatrix} \quad (5)$$

The elements k and δ are usually given by the connected networks, but it is possible to adjust them by inserting a transformer at one side. This allows to influence the system matrix **A**.
Even if it is not the major objective to control the reactive consumption ΔQ of the DIPFC it is tried to influence it by choosing $\underline{V}_i$ and $\underline{V}_k$ somehow.

The parameters k and δ should be selected in a way that the reactive-power consumption of this FACTS device is delivered in equal parts of both networks. This can be described by:

$$Q_i = -Q_k \quad (6)$$

In equation (6) it is considered, that the currents are counted from side i to k. The calculation of the reactive-power flow on the right network yields:

$$Q_k = 3V_i^2 k\left(-\cos\left(\delta-\frac{2\pi}{3}\right)+k \quad -\cos\left(\delta+\frac{2\pi}{3}\right)+k\right)\begin{pmatrix}B_1\\B_2\end{pmatrix} \quad (7)$$

Equation (6) is fulfilled when the two requirements

$$-1+k\cos\left(\frac{2\pi}{3}-\delta\right) = k\cos\left(\delta-\frac{2\pi}{3}\right)-k^2 \quad (8)$$

$$-1+k\cos\left(\frac{2\pi}{3}+\delta\right) = k\cos\left(\delta+\frac{2\pi}{3}\right)-k^2 \quad (9)$$

are satisfied. The both requirements yield to:

$$1 = k^2 \;\Rightarrow\; k = \pm 1 \quad (10)$$

Equation (10) shows that the demand of equal reactive-power supply can be fulfilled if the amplitudes of the both connection voltages are equal. The load angle δ in contrast has no influence. The parameter k will be defined to:

$$k = 1 \quad (11)$$

Now the parameter δ can be optimized. Therefore equation (5) is considered again.

$$\begin{aligned}\begin{pmatrix}P_i\\Q_i\end{pmatrix} &= 3V_i^2\begin{pmatrix}a_{11} & a_{12}\\ a_{21} & a_{22}\end{pmatrix}\begin{pmatrix}B_1\\B_2\end{pmatrix} =\\ &= 3V_i^2\left(\begin{pmatrix}a_{11}\\a_{21}\end{pmatrix}B_1+\begin{pmatrix}a_{12}\\a_{22}\end{pmatrix}B_2\right) =\\ &= 3V_i^2\left(\mathbf{V}_1B_1+\mathbf{V}_2B_2\right)\end{aligned} \quad (12)$$

The vector of P_i and Q_i is, neglecting $3V_i^2$, built up by the addition of, with the suszeptances weighted, vectors $\mathbf{V}_1$ and $\mathbf{V}_2$.
In figure 4 the two columns of the matrix **A** are interpreted as two-dimensional vectors $\mathbf{V}_1$ and $\mathbf{V}_2$ within the complex $P_i - Q_i$ – layer.

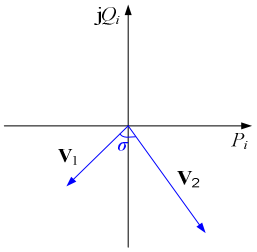

Fig. 4: Transmission vectors of the system matrix **A**

An optimum would be achieved when the two vectors are orthogonal to each other. That means, that the angle

$$\sigma = \arccos\left(\frac{\mathbf{V}_1\mathbf{V}_2}{|\mathbf{V}_1|\cdot|\mathbf{V}_2|}\right) \qquad (13)$$

is equal to 90 degrees. In figure 5 the angle σ is depicted as a function of the load angle δ.

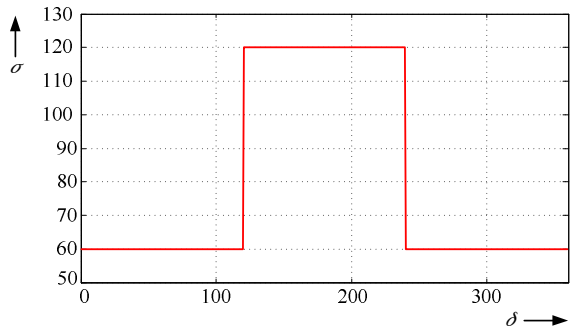

Fig. 5: Angle between $\mathbf{V}_1$ and $\mathbf{V}_2$ as function of δ

It can be seen, that there is no angle where the both vectors are orthogonal. Therefore another criteria has to be found to optimize δ.
Again the reactive-power consumption of the DIPFC is considered

$$\Delta Q = 6V_i^2\left(\cos\left(\frac{2\pi}{3}-\delta\right)-1 \quad \cos\left(\frac{2\pi}{3}+\delta\right)-1\right)\begin{pmatrix}B_1\\B_2\end{pmatrix} \qquad (14)$$

and it is assumed that $B_1 = -B_2$, which means that one module operates inductive and the other capacitive with the same value. Figure 6 shows that $\Delta Q = 0$ for a load angle of $\delta = \pi$.

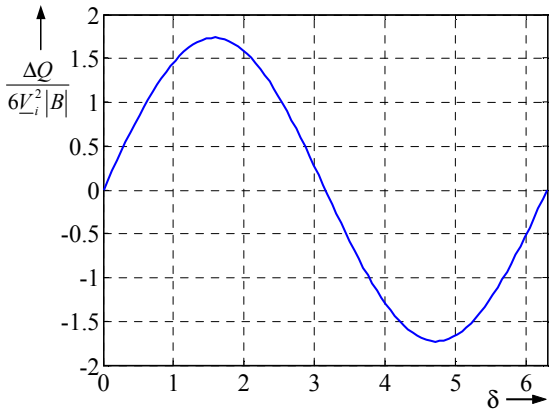

Fig. 6: Reactive-power consumption of the DIPFC with module values of $B_1 = -B_2$

Therefore k=1 and δ=π are optimal parameters for an active-power exchange between the two connected networks.

Because the DIPFC is realized as a model at the network demonstration model (DDM) of the Institute of Electrical Power Systems at the Friedrich - Alexander - University of Erlangen - Nürnberg, the following calculation values correspond to the values in table 1.

open-circuit voltages	
$\underline{V}_{pi} = 140.5\text{V}$	$\underline{V}_{pk} = 140.5\text{V}\cdot e^{j\pi}$
short-circuit impedances	
$\underline{Z}_i = (1.287 + j7.378)\,\Omega$	$\underline{Z}_k = (1.346 + j5.526)\,\Omega$
module parameters	
$L = 80\text{mH}$ $C = 50\mu\text{F}$	$X_L = 25.13\Omega$ $X_C = 63.66\Omega$
resulting system matrix **A**	
$\mathbf{A} = \begin{pmatrix} 0.866 & -0.866 \\ -0.5 & -0.5 \end{pmatrix}$	
model scale of voltage and current	
$m_V = 1000$	$m_c = 100$
nominal power of the model: 1.9 kVA	

Tab. 1: Parameters of the investigated DIPFC

Figure 7 depicts the operating area of the DIPFC with the used parameters from table 1. It can easily be seen that the active- and reactive power can be exchanged independently.

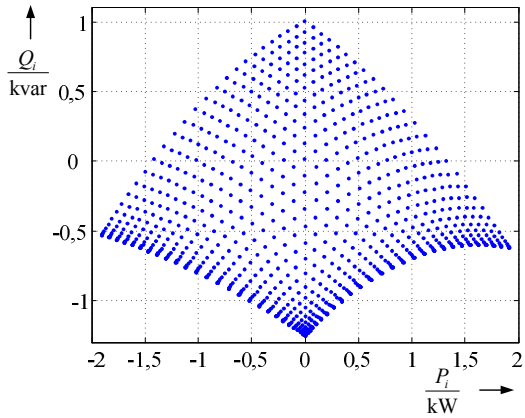

Fig. 7: Operating range of the investigated DIPFC

4. Dynamic modelling of the DIPFC behaviour

In a first step a Matlab/Simulink model of the considered DIPFC structure is introduced which directly reproduces the switching actions of the applied thyristors in a realistic way. This model is named "Hardware–Model". Afterwards the main problem is to develop a "System–Model" consisting of linear transfer functions which describes the dynamic behaviour of the Hardware–Model. In this paper the suggested solution is to define the fundamental component susceptances of the modules as dynamic variables. After a linearization of the non-linear behaviour between the ignition angle of the thyristors and the fundamental component susceptance by suitable means the demanded System–Model can be formed. The parameters of the transfer functions are obtained by a comparison of the step responses of the fundamental component susceptances of the two introduced Simulink models.

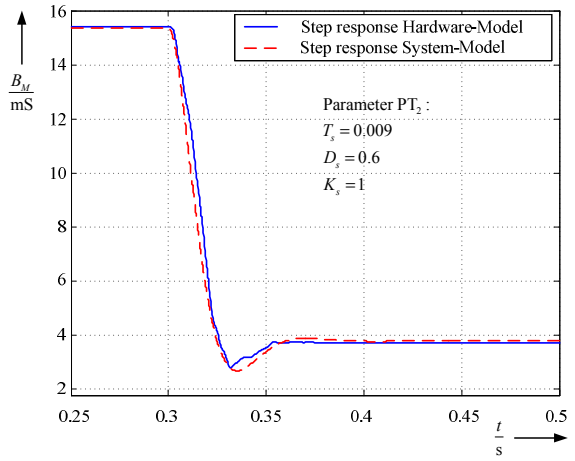

Fig. 8: Comparison of the step responses of the introduced Simulink models

Figure 8 depicts this comparison of the step responses as a function of the simulated time.
The PT_2-transfer function

$$F_S(s) = \frac{K_S}{1 + 2D_S T_S s + T_S^2 s^2} \tag{15}$$

with: $D_S = 0.6, T_S = 0.009$ and $K_S = 1$

was found empirically.

5. Controller Design

Figure 9 shows a block diagram of the controlled system completed with a closed–loop controller. F_{S1} and F_{S2} refer to the transfer functions of module 1 respectively module 2 while R_{11} to R_{22} refer to the proposed controller. The elements a_{11} to a_{22} represent the system matrix **A**.
The block diagram shows that the resulting structure is a coupled system which means that one deals with a multi-variable control problem. The two controlled variables (active- and reactive power) are both being influenced by the actuating variables (B_1, B_2) which are described by the transfer functions F_{S1} and F_{S2}. The proposed controller which is also switched in a coupled way is subsequently designed to eliminate the couplings of the controlled system. The theory of multi-variable control points out the necessary method of resolution for the independent control of active- and reactive power. The available linear transfer functions of the controlled system make it possible to calculate transfer functions for the controller which decouple the investigated system. Therefore the system disintegrates into two independent control systems which can be designed separately.
The transfer function of the decoupled system yields to:

$$\begin{pmatrix} P_i \\ Q_i \end{pmatrix} = V \begin{pmatrix} a_{11}F_{S1}G_{K1} & 0 \\ 0 & a_{22}F_{S2}G_{K2} \end{pmatrix} \begin{pmatrix} e_1 \\ e_2 \end{pmatrix} \tag{16}$$

The open-loop transfer function of the original system can be described through:

$$\begin{pmatrix} P_i \\ Q_i \end{pmatrix} = V \begin{pmatrix} a_{11}F_{S1}R_{11} + & a_{11}F_{S1}R_{12} + \\ +a_{12}F_{S2}R_{21} & +a_{12}F_{S2}R_{22} \\ a_{21}F_{S1}R_{11} + & a_{21}F_{S1}R_{12} + \\ +a_{22}F_{S2}R_{21} & +a_{22}F_{S2}R_{22} \end{pmatrix} \begin{pmatrix} e_1 \\ e_2 \end{pmatrix} \tag{17}$$

with: $V = 3V_i^2$

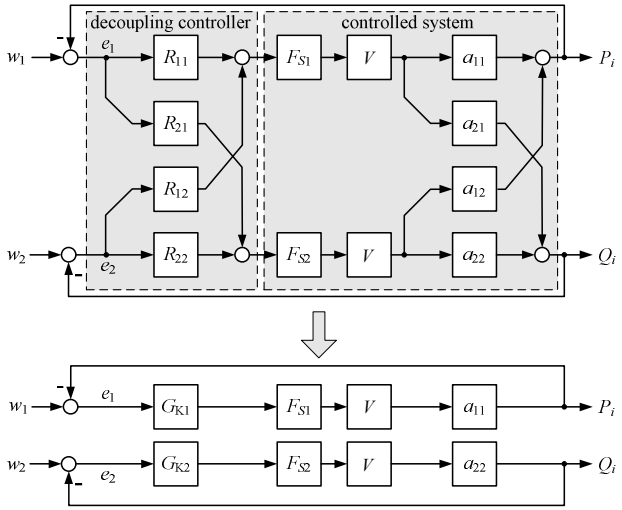

Fig. 9: Block diagram of the resulting controlled structure

By comparing the elements of equation (16) and (17) the following relation can be found.

$$R_{12} = -\frac{a_{12}F_{S2}}{a_{11}F_{S1}} R_{22} \quad \text{and} \quad R_{21} = -\frac{a_{21}F_{S1}}{a_{22}F_{S2}} R_{11} \tag{18}$$

A substitution of equation (18) in (17) gives:

$$\begin{pmatrix} P_i \\ Q_i \end{pmatrix} = V \begin{pmatrix} \frac{\det(\mathbf{A})}{a_{22}} F_{S1}R_{11} & 0 \\ 0 & \frac{\det(\mathbf{A})}{a_{11}} F_{S2}R_{22} \end{pmatrix} \begin{pmatrix} e_1 \\ e_2 \end{pmatrix} \tag{19}$$

Where $\det(\mathbf{A})$ is the determinant of the system matrix.
The open-loop transfer functions of the decoupled control loop can be described as:

$$F_{o\nu}(s) = a_{\nu\nu} V F_{S\nu}(s) G_{K\nu}(s) \tag{20}$$

If the modules are - as mentioned - simulated as PT_2-elements and the controllers are realized as PI-controllers, equation (20) yields to:

$$F_{o\nu}(s) = a_{\nu\nu} V \frac{1}{1 + 2D_{s\nu}T_{s\nu}s + T_{s\nu}^2 s^2} \cdot K_{R\nu} \frac{1 + sT_{R\nu}}{s} \tag{21}$$

It follows the closed-loop control as:

$$F_{K\nu}(s) = \frac{(1 + T_{R\nu}s)}{1 + \frac{(1 + K'_{R\nu}T_{R\nu})}{K'_{R\nu}} s + \frac{2D_{S\nu}T_{S\nu}}{K'_{R\nu}} s^2 + \frac{T_{S\nu}^2}{K'_{R\nu}} s^3} \tag{22}$$

with: $K'_{Rv} = a_{vv} V K_{Rv}$

If the damping factor D_S is smaller than 1 (as it is given in the investigated system) the analysis of the denominator of equation (22) yields to 3 eigenvalues. One of these only consists of a real part while the other 2 always form a conjugated complex pair of eigenvalues. With the parameters of the controller K_R and T_R the position of these eigenvalues within the complex area can be influenced. For an optimally adjusted controller of the DIPFC, the real parts of the eigenvalues a should be equal, in order that all transients in the system are damped equally. For given parameters of the transfer function of the modules the real part of the eigenvalues can be calculated.

$$a = \frac{2D_s}{3T_s} \tag{23}$$

As equation (23) shows, a is only a function of D_s and T_s. But it has to be considered, that the PT_2-element has to be found empirically and depends very well from all system parameters.
If the quadratic term of the PT_2-element of the controlled system is neglected, the time constant T_R of the controller can compensate the residual time constant. To fulfill the requirement of equal real parts for all eigenvalues the gain factor K'_R has to be set to:

$$K'_R = \frac{2T_s^2 a^2 - 1}{T_R - \frac{1}{a}} \tag{24}$$

With these parameters of the controller, the requirement to an equal real part of the eigenvalues can be fulfilled.

A comparison of equation (19) with (20) yields:

$$V \frac{\det(\mathbf{A})}{a_{\mu\mu}} F_{S\nu}(s) R_{\nu\nu}(s) = a_{\nu\nu} V F_{S\nu}(s) G_{K\nu}(s) \tag{25}$$

Equation (25) converted to $R_{\nu\nu}$ gives the transfer function of the controller.

$$R_{\nu\nu}(s) = \frac{a_{\nu\nu} a_{\mu\mu}}{\det(\mathbf{A})} G_{K\nu}(s) \tag{26}$$

As the time constants of the controller are determined, the gains can be calculated with equation (24) and (26) to:

$$K_P = \frac{a_{22}}{V \det(\mathbf{A})} K'_{R1} \quad \text{and} \quad K_Q = \frac{a_{11}}{V \det(\mathbf{A})} K'_{R2} \tag{27}$$

6. Results

6.1 Behaviour of the controlled variables

The designed controller leads to a highly dynamic behaviour of the controlled variables. Active- and reactive power can be controlled independently to any value couple within the range of operation (Fig. 7) of the DIPFC. Figure 10 depicts the incoming active- and reactive power as a function of the simulated time. One of the controlled variables follows a reference value step while the reference value of the other variable isn't changed. The figure makes clear that the closed-loop system behaves very dynamically. Especially if it is kept in mind, that the thyristors are fired only once per period, which means that there can be a dead time up to 20ms (for a 50Hz network). Intense oscillations around the demanded reference values don't occur as a result of the optimized controller parameters.
Moreover the occurring not fully eliminated couplings are examined and can be led back to necessary neglects during the modelling process.

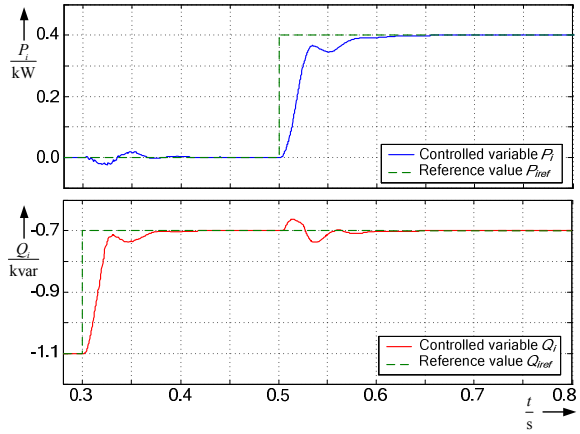

Fig. 10: Active- and reactive power as functions of the simulated time

6.2 Disturbance behaviour

Afterwards the disturbance behaviour of the developed closed-loop controlled system is analyzed. As disturbances changes in magnitude and phase of the incoming and outgoing voltage are considered.
The graphs in Figure 11 show the simulation results when the load angle is changed from 180° to 170° at the time of t=0.5s and is set back at t=0.8s.

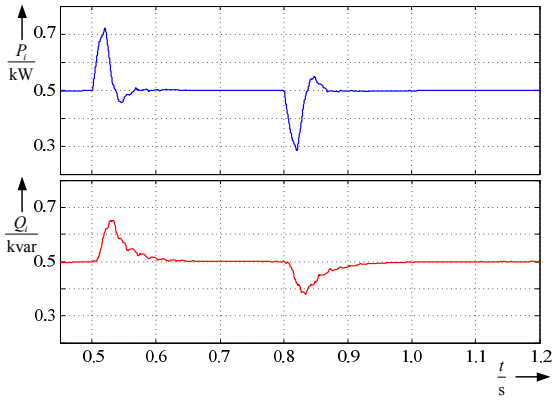

Fig. 11: System response by sudden change of the load angle δ

The results of this investigation illustrate that also impacts of disturbances are damped sufficiently. A sudden voltage rise shows similar results.

6.3 Behaviour in fault case

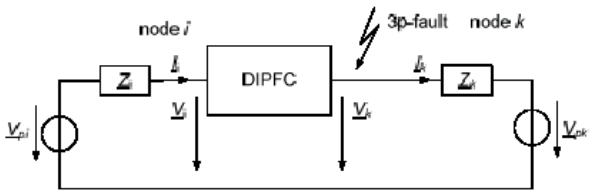

Fig. 12: 3-phase fault at node *k*

The designed controller for the DIPFC is not only used to influence the load flow over the considered transmission line but has also the additional task to react to fault cases. In this paper the possibility of a short circuit current limitation by means of a DIPFC is presented. The Hardware-Model is extended with a short circuit detection function. In case of a detected fault the DIPFC has the task to limit the short circuit current over the transmission line. In order to achieve this, the fundamental component susceptances of the two DIPFC modules are controlled to the operation point B_1=B_2=0. Figure 12 depicts the circuit diagram of a 3-phase fault at the node *k*. The simulation shows that the incoming short-circuit current at node *i* can be limited in a highly dynamic way. Figure 13 presents the complex space phasor of the short-circuit current at node *i*. The magnitude of the stationary space phasor in short circuit case can be limited to values which are even smaller than magnitudes of normal load flow conditions.

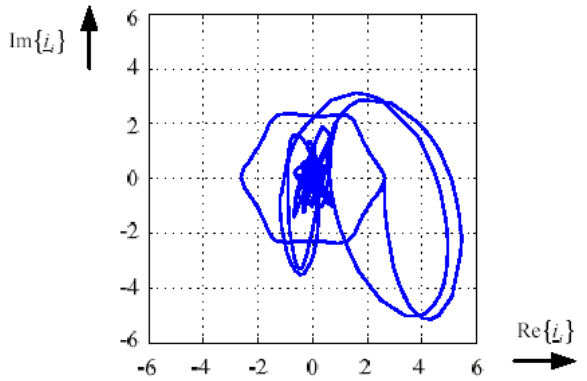

Fig. 13: Complex space phasor of the short circuit current at node *i*

7. Conclusion

The presented paper describes the development of a closed-loop power control for a Dynamic Interphase Power Flow Controller with two controlled modules. The dynamic modelling of the DIPFC leads to a linear system description, the System-Model. Based on this System-Model a controller can be designed which decouples the two controlled variables. The chosen structures for the controllers of the decoupled systems are PI–controllers. Even though a PID structure would be more optimal the PI type is chosen in view of the realization of the designed controller at the network demonstration model. The optimal parameters for the PI–controllers are calculated based on the analysis of the eigenvalues of the controlled system which match with the eigenvalues of the investigated dynamic fundamental component susceptances in this case. As result the active- and reactive-power flow over the considered transmission line can be controlled independently. Moreover the optimisation of controller parameters results in a highly dynamic system behaviour. Finally the designed controller is extended with a short circuit current limitation system.

References

[1] Herold, G., Ebner, G., Süßbrich, R., Weindl, Ch.: Comparison of Different Calculation Methods for a Power Semiconductor Based Interphase Power Flow Controller, 2003 *IEEE Bologna Power Tech Conference*, 23.-26. Juni 2003, Bologna (Italien), Report BPT03-105

[2] Ebner, G.; Herold, G.: Controlled active- and reactive-power flow using a DIPFC, *11th European Conference on Power Electronics and Applications*, 11.-14. September 2005, Dresden (Germany), Bericht 181

[3] Weindl Ch.; Herold G.; Ebner G.; Süßbrich R.: Beschreibung und Berechnung eines dynamischen Zwischenphasenreglers. Teil I: Systembeschreibung - Analyse der Schaltzustände & Ableitung der Ersatznetzwerke, *ELEKTRIE 58* (2004), Nr. 1-12, S. 9-19

[4] Weindl Ch.; Herold G.; Ebner G.; Süßbrich R.: Beschreibung und Berechnung eines dynamischen Zwischenphasenreglers. Teil II: Analytisches Lösungsverfahren - Beispielstudie, *ELEKTRIE 58* (2004), Nr. 1-12, S. 20-29

[5] Christl N., Lützelberger P., Sadek K.: Geregelter Serienkompensator für Lastflußregelung und Überstrombegrenzung, *etz Band 115* (1994) Heft 11

[6] Bohmann L. J.; Lasseter R. H.:Stability and Harmonics in Thyristor Controlled Reactors, *IEEE Transactions on Power Delivery*, Vol. 5, No. 2, April 1990

[7] Brochu J., Pelletier P., Beauregard F., Morin G.: The Inter-phase Power Controller. A New Concept for Managing Power Flow Within AC Networks, *IEEE Transmission and Distribution, Manuscript of the 1993 Summer Meeting in Vancouver*

[8] Habashi K., Lombard J., Mourad S., Pelletier P., Morin G., Beauregard, F., Brochu, J.; The Design of a 200 MW Inter-phase Power Controller Prototype, *IEEE Transmission and Distribution, Manuscript of the 1993 Summer Meeting in Vancouver*

[9] Hingorani N.G.: Understanding FACTS, Concepts and Technology of Flexible AC Transmission System, *IEEE Press, New York*